

PARAMETER-EFFICIENT FINE-TUNING VIA CIRCULAR CONVOLUTION

Aochuan Chen[†] Jiashun Cheng[†] Zijing Liu^{idea} Ziqi Gao[†] Fugee Tsung[†] Yu Li^{idea} Jia Li[†]

[†]The Hong Kong University of Science and Technology (Guangzhou)

^{idea}International Digital Economy Academy

ABSTRACT

Low-Rank Adaptation (LoRA) has gained popularity for fine-tuning large foundation models, leveraging low-rank matrices \mathbf{A} and \mathbf{B} to represent weight changes (*i.e.*, $\Delta\mathbf{W} = \mathbf{B}\mathbf{A}$). This method reduces trainable parameters and mitigates heavy memory consumption associated with full delta matrices by sequentially multiplying \mathbf{A} and \mathbf{B} with the activation. Despite its success, the intrinsic low-rank characteristic may limit its performance. Although several variants have been proposed to address this issue, they often overlook the crucial computational and memory efficiency brought by LoRA. In this paper, we propose Circular Convolution Adaptation (C^3A), which not only achieves high-rank adaptation with enhanced performance but also excels in both computational power and memory utilization. Extensive experiments demonstrate that C^3A consistently outperforms LoRA and its variants across various fine-tuning tasks.

1 INTRODUCTION

In recent years, Large Foundation Models (LFMs) have surged in popularity due to their remarkable performance across various tasks in natural language processing (NLP) Brown et al. (2020); Touvron et al. (2023), computer vision (CV) Radford et al. (2021); Kirillov et al. (2023), and other domains Li et al. (2024). Characterized by their vast number of parameters and substantial computational demands, these models have set new benchmarks in accuracy and versatility. However, their size and complexity pose significant challenges for efficient fine-tuning, particularly in resource-constrained environments Malladi et al. (2023); Zhang et al. (2024b). To address this issue, Parameter-efficient fine-tuning (PEFT) techniques Mangrulkar et al. (2022), such as Low-Rank Adaptation (LoRA) Hu et al. (2021), have emerged as outstanding practical solutions.

LoRA reduces the number of trainable parameters by employing low-rank matrices to approximate weight changes, making fine-tuning more feasible and accessible without compromising the model’s performance. Concretely, LoRA can be expressed in math:

$$\mathbf{W}\mathbf{x} = (\mathbf{W}_0 + \Delta\mathbf{W})\mathbf{x} = \mathbf{W}_0\mathbf{x} + \mathbf{B}(\mathbf{A}\mathbf{x}),$$

where $\mathbf{W}, \mathbf{W}_0, \Delta\mathbf{W} \in \mathbb{R}^{d_1 \times d_2}$ are weight matrices, $\mathbf{B} \in \mathbb{R}^{d_1 \times r}$, $\mathbf{A} \in \mathbb{R}^{r \times d_2}$ are low-rank matrices to construct $\Delta\mathbf{W}$ and $\mathbf{x} \in \mathbb{R}^{d_2}$ is the activations. The number of trainable parameters is $r(d_1 + d_2)$, prompting the choice $r \ll \min(d_1, d_2)$ (*e.g.*, $r = 8$ for

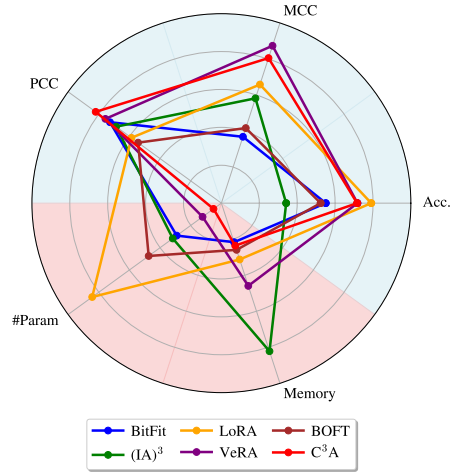


Figure 1: Relative comparison of C^3A and baselines on RoBERTa-Base. The Pearson Correlation Coefficient (PCC) is evaluated on STS-B and the Matthew’s Correlation Coefficient (MCC) on CoLA. Accuracies across SST-2, MRPC, QNLI, and RTE are averaged and reported as Acc. #Param denotes the count of learnable parameters (excluding the head), while Memory indicates the peak GPU memory usage during training. Metrics highlighted in blue represent values where higher is better, and those in red indicate values where lower is better. Refer to Table 2 for absolute statistics.

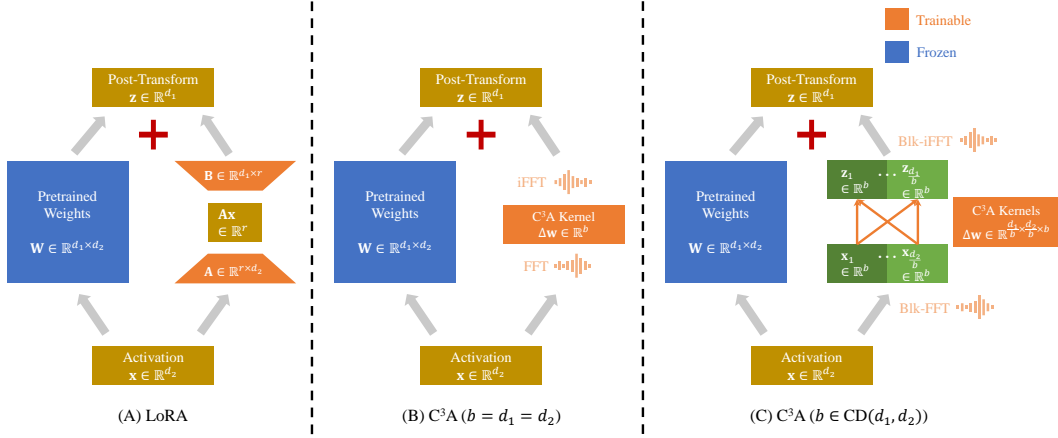


Figure 2: **Overview of LoRA (A) and our C³A (B,C) method.** In LoRA, only low-rank matrices **A** and **B** are trained and the delta weight is represented by their product (*i.e.*, $\Delta\mathbf{W} = \mathbf{BA}$). The total trainable parameter number is $r(d_1 + d_2)$, which is associated with the rank of the delta weight. In C³A, circular convolution kernels $\Delta\mathbf{w}$ are tuned to adapt to the downstream task and the delta weight is represented by the (block-)circular matrix they construct (*i.e.*, $\Delta\mathbf{W} = \mathcal{C}_{(\text{blk})}(\Delta\mathbf{w})$). The total trainable parameter count is $\frac{d_1 d_2}{b}$, which disentangles with the rank of the delta weight. Here, b is the block size of the block-circular matrix and it should be a common divisor (CD) of d_1 and d_2 .

$d_1 = d_2 = 1024$) for achieving high parameter efficiency. However, as discussed in Zeng & Lee (2023), LoRA’s capacity to represent a target model is strictly limited by r . To address this trade-off between performance and efficiency, Kopiczko et al. (2023) proposed Vector Random Matrix Adaptation (VeRA), which achieves competitive performance with significantly fewer trainable parameters through fixed random-matrix projections. Despite its low parameter count, VeRA requires substantial computational power and memory due to the large size of the random matrices used for projection. This raises the following open research question in the context of PEFT:

How can high-rank adaptation be achieved without incurring significant costs in terms of time complexity, memory usage, and trainable parameters?

As discussed in Dosovitskiy et al. (2020), dense linear layers lack inductive biases, which poses challenge on the optimization process and therefore limits transformers’ ability to compete with Convolutional Neural Networks (CNNs) when data is scarce. Given the constraints of a small training set for the downstream task, we posit that incorporating a stronger inductive bias could improve the adaptation performance. In light of this, we propose Circular Convolution Adaptation (C³A), featuring the circular convolution operator Bamieh (2018).

Circular convolution has been famous in signal processing Li et al. (2020) and cryptography Dworkin et al. (2001) for its distinguished efficiency and compactness. This operator can be equivalently represented as multiplication by a circulant matrix, which offers rank flexibility that is unconstrained by the number of trainable parameters. Moreover, leveraging the Fast Fourier Transform (FFT), C³A ensures better time and memory efficiency than directly multiplying the circulant matrix Bamieh (2018), rendering it competitive with LoRA from the efficiency aspect. In a word, circular convolution is a promising option for escaping the rank curse of LoRA at minimal cost. We summarize our contribution as follows:

- ① We introduce C³A, a novel approach for PEFT using convolution. This method leverages the circular convolution operation and its equivalent circulant matrix to provide a flexible rank, which is free of linear constraint by the number of trainable parameters, for the delta matrix.
- ② Leveraging the elegant diagonalization of the circulant matrix, we implement both the forward pass and backpropagation using FFT. With the incorporation of FFT, the computation and memory efficiency of C³A excels. C³A strikes a unique balance between performance and efficiency.

③ To offer greater flexibility in controlling the number of trainable parameters, we extend C³A by incorporating block-circular convolution, which results in block-circulant matrices. This extension allows C³A to achieve fully customizable parameter counts as well as adaptable rank configurations.

④ We validate C³A through comprehensive fine-tuning experiments across diverse tasks including natural language understanding, instruction tuning and image classification. Experiments demonstrate C³A’s outstanding accuracy and memory merits compared to existing state-of-the-art methods.

2 RELATED WORK

2.1 PARAMETER-EFFICIENT FINE-TUNING

Research on Parameter-Efficient Fine-Tuning (PEFT) has generally progressed along three main directions. The first direction involves partially updating the pre-trained neural network (*e.g.*, the body Oh et al. (2020) or the biases Zaken et al. (2021)). Traditional methods relied on hand-crafted heuristics Han et al. (2015); Oh et al. (2020) to identify which parameters are crucial and should be fine-tuned. More advanced approaches employ optimization techniques Guo et al. (2020); Xu et al. (2021); Fu et al. (2023). For example, Guo et al. (2020) reformulated such a discrete optimization problem into a continuous one by employing Bernoulli masks and the Gumbel-softmax approximation.

The second direction emerged to maintain the integrity of the pre-trained model while enabling a high degree of parameter sharing through adapter-based methods He et al. (2021); Rebuffi et al. (2017); Rücklé et al. (2020); Liu et al. (2022). These works focus on integrating additional modules, termed adapters, to fit the downstream task, effectively decoupling the pre-trained model parameters from those specific to the downstream task. Prompt Tuning Brown et al. (2020); Gao et al. (2020); Chen et al. (2023); Zhang et al. (2024a) and Prefix Tuning Li & Liang (2021) also fall into this category, despite ignoring potential semantic meanings.

The final direction is characterized by delta-weight-based methods, such as Low-Rank Adaptation (LoRA) Hu et al. (2021) and Orthogonal Fine-tuning (OFT) Qiu et al. (2023). These methods bridge the gap between the pre-trained model and the downstream task by adaptive delta weights, which are stored separately while used in combination with the pre-trained weights. This unique design enables disentanglement of the pretrained and downstream-specific weights. Namely, it achieves parameter sharing and preserves the ability to integrate without additional inference cost. LoRA models the delta-weights by an additive matrix while OFT does it by a multiplicative one. To further improve either parameter efficiency or performance, many variants has been proposed for both of the methods Kopiczko et al. (2023); Liu et al. (2024; 2023); Yuan et al. (2024). However, these methods can hardly achieve high parameter efficiency and performance without incurring heavy computation and memory usage.

2.2 CIRCULAR CONVOLUTION

Circular convolution has been extensively studied in signal processing Rabiner et al. (1978); McGillem & Cooper (1984); Li et al. (2020) and cryptography Dworkin et al. (2001); Gong et al. (2024). Owing to its computational advantages, circular convolution has also been explored in machine learning for generating long embeddings of high-dimensional data Yu et al. (2014) and compressing heavily parameterized layers Cheng et al. (2015); Ding et al. (2017). Remarkably, it achieves these efficiencies without significant performance degradation, which makes it a promising technique for fine-tuning applications.

Despite its success in small neural networks such as LeNet Cheng et al. (2015), circular convolution has not demonstrated lossless performance in modern large foundational models (LFMs) or even in their base architecture, the transformer. This limitation may be attributed to the conflict between its high intrinsic bias (*i.e.*, the circulant pattern) and the vast amount of data required for training LFMs. Conversely, when fine-tuning LFMs, it is often impractical to collect as much data as needed for training from scratch. In such scenarios, the intrinsic bias of circular convolution could potentially serve as a regularization mechanism, thereby benefiting the optimization process of fine-tuning.

3 METHOD

In this section, we present C³A (see an overview in Figure 2), a novel PEFT approach based on the circular convolution. C³A follows LoRA’s setting of learning an additive linear operation over the original dense linear transformation. However, instead of using low-rank decomposition and the matrix multiplication operator, C³A resorts to circular convolution as this additive linear operation. Section 3.1 introduces the notations we use. Section 3.2 discusses the circular convolution operator, its equivalent circulant matrix, and its calculation in the frequency domain. Section 3.3 details an efficient method for backpropagation. Section 3.4 describes block-wise convolution for controlling the number of trainable parameters. Finally, Section 3.5 analyzes the computational complexity.

3.1 NOTATIONS

The adapted weight matrix, the original weight matrix, and the delta matrix are denoted by \mathbf{W} , \mathbf{W}_0 , and $\Delta\mathbf{W}$, respectively ($\mathbf{W}, \mathbf{W}_0, \Delta\mathbf{W} \in \mathbb{R}^{d_1 \times d_2}$). The activation vector of the previous layer is denoted by $\mathbf{x} \in \mathbb{R}^{d_2}$. The post-transformation vector is \mathbf{z} , where $\mathbf{z} = \mathbf{W}\mathbf{x} \in \mathbb{R}^{d_1}$, and the incremental part is denoted by $\Delta\mathbf{z}$, where $\Delta\mathbf{z} = \Delta\mathbf{W}\mathbf{x} \in \mathbb{R}^{d_1}$. The matrices \mathbf{A} and \mathbf{B} are low-rank matrices introduced by LoRA to represent $\Delta\mathbf{W}$, with r being their rank. r_v specifies the rank of the random projection matrix used in VeRA. The circular convolution kernel of C³A is denoted by $\Delta\mathbf{w}$ and the circular convolution operator by \star . The loss function is represented by \mathcal{L} . The Fast Fourier Transform and its inverse are denoted by FFT and iFFT, respectively. The Hadamard product is denoted by \circ .

3.2 CIRCULAR CONVOLUTION

Firstly, for simplicity, we assume $d_1 = d_2 = d$ and $\Delta\mathbf{w} \in \mathbb{R}^d$. The circular convolution operator is defined as $\Delta\mathbf{z} = \Delta\mathbf{w} \star \mathbf{x} = \mathcal{C}(\Delta\mathbf{w})\mathbf{x}$, where $\mathcal{C}(\cdot)$ is a function which takes a vector and outputs the corresponding circulant matrix. Concretely, the first row of $\mathcal{C}(\Delta\mathbf{w})$ is $\Delta\mathbf{w}$ and the following rows are equal to the row above them periodically shifted to the right by one element. In math,

$$\mathcal{C}(\Delta\mathbf{w}) = \begin{bmatrix} \Delta w_1 & \Delta w_2 & \cdots & \Delta w_{d-1} & \Delta w_d \\ \Delta w_d & \Delta w_1 & \cdots & \Delta w_{d-2} & \Delta w_{d-1} \\ \cdots & \cdots & \cdots & \cdots & \cdots \\ \Delta w_3 & \Delta w_4 & \cdots & \Delta w_1 & \Delta w_2 \\ \Delta w_2 & \Delta w_3 & \cdots & \Delta w_d & \Delta w_1 \end{bmatrix}.$$

Theoretically, the rank of $\mathcal{C}(\Delta\mathbf{w})$ is given by $d - \text{Deg}(\text{gcd}(f(x), x^d - 1))$ Ingleton (1956), where $\text{Deg}(\cdot)$ denotes the degree of a polynomial, $f(x)$ is the polynomial associated with $\Delta\mathbf{w}$ (i.e., $f(x) = \sum_{i=1}^d \Delta w_i x^{i-1}$), and $\text{gcd}(\cdot)$ represents the greatest common divisor. Consequently, the theoretical upper bound on the rank of $\mathcal{C}(\Delta\mathbf{w})$ is d . By learning $\Delta\mathbf{w}$ in the \mathbb{R}^n oracle, C³A automatically achieves dynamic rank selection, which is not linearly constrained by the number of learnable parameters, unlike LoRA.

To achieve high efficiency, we leverage the beautiful circulant structure of $\mathcal{C}(\Delta\mathbf{w})$, which makes it diagonalizable by the Fourier basis (\mathbf{F}). In math, it can be described as $\mathcal{C}(\Delta\mathbf{w}) = \mathbf{F} \frac{\Lambda}{d} \mathbf{F}^{-1}$ Golub & Van Loan (1996), where Λ is its eigenvalues and can be calculated by a Fourier transform of the first row (i.e., $\Lambda = \text{diag}(\mathbf{F}\Delta\mathbf{w})$). Therefore, we can calculate $\Delta\mathbf{w} \star \mathbf{x}$ as

$$\begin{aligned} \Delta\mathbf{w} \star \mathbf{x} &= \mathbf{F} \text{diag}\left(\frac{\mathbf{F}\Delta\mathbf{w}}{d}\right) \mathbf{F}^{-1} \mathbf{x} \\ &= \text{FFT}(\text{FFT}(\Delta\mathbf{w}) \circ \text{iFFT}(\mathbf{x})). \end{aligned} \tag{1}$$

3.3 BACKPROPAGATION

To implement backpropagation efficiently, we require the analytical derivatives of the loss function \mathcal{L} , with respect to $\Delta\mathbf{w}$ and \mathbf{x} . Utilizing the chain rule, these derivatives can be expressed as:

$$\frac{\partial \mathcal{L}}{\partial \mathbf{x}} = \frac{\partial \Delta\mathbf{z}}{\partial \mathbf{x}} \frac{\partial \mathcal{L}}{\partial \Delta\mathbf{z}}, \quad \frac{\partial \mathcal{L}}{\partial \Delta\mathbf{w}} = \frac{\partial \Delta\mathbf{z}}{\partial \Delta\mathbf{w}} \frac{\partial \mathcal{L}}{\partial \Delta\mathbf{z}}. \tag{2}$$

Since $\Delta \mathbf{z} = \mathcal{C}(\Delta \mathbf{w})\mathbf{x}$, it follows that $\frac{\partial \Delta \mathbf{z}}{\partial \mathbf{x}} = \mathcal{C}(\Delta \mathbf{w})$. For $\frac{\partial \Delta \mathbf{z}}{\partial \Delta \mathbf{w}}$, we note that the circular convolution operation is commutative (i.e., $\mathcal{C}(\Delta \mathbf{w})\mathbf{x} = \mathcal{C}(\mathbf{x})\Delta \mathbf{w}$), thus $\frac{\partial \Delta \mathbf{z}}{\partial \Delta \mathbf{w}} = \mathcal{C}(\mathbf{x})$. Substituting these results into Equation 2, we obtain:

$$\frac{\partial \mathcal{L}}{\partial \mathbf{x}} = \mathcal{C}(\Delta \mathbf{w}) \frac{\partial \mathcal{L}}{\partial \Delta \mathbf{z}}, \quad \frac{\partial \mathcal{L}}{\partial \Delta \mathbf{w}} = \mathcal{C}(\mathbf{x}) \frac{\partial \mathcal{L}}{\partial \Delta \mathbf{z}}.$$

These expressions can also be interpreted as circular convolutions:

$$\frac{\partial \mathcal{L}}{\partial \mathbf{x}} = \Delta \mathbf{w} \star \frac{\partial \mathcal{L}}{\partial \Delta \mathbf{z}}, \quad \frac{\partial \mathcal{L}}{\partial \Delta \mathbf{w}} = \mathbf{x} \star \frac{\partial \mathcal{L}}{\partial \Delta \mathbf{z}}.$$

By explicitly implementing this derivative calculation using Equation 1, backpropagation can also enjoy the computational efficiency provided by the FFT algorithm.

3.4 BLOCK-CIRCULAR CONVOLUTION

Despite the elegance and efficiency of the circular convolution operator, it has 2 fundamental limitations due to the requirement that the convolution kernel must be the same size as the activation vector: ❶ *It cannot be applied to non-square weight matrices.* ❷ *The number of learnable parameters cannot be altered.* The first limitation restricts its application in scenarios such as fine-tuning a LLaMA3-8B model, where the weight matrix sizes include 4096×1024 . The second limitation reduces the flexibility of C³A, making it challenging to handle complex downstream tasks that require a larger number of learnable parameters. To address these limitations, we resort to block-circular convolution. By splitting the activation vector \mathbf{x} and the post-transformation vector \mathbf{z} into blocks of the same size, we can assign unique convolution kernels to each pair of these blocks. To be concrete,

$$\mathbf{x} = \begin{bmatrix} \mathbf{x}_1 & \mathbf{x}_2 & \cdots & \mathbf{x}_{\frac{d_2}{b}} \end{bmatrix}, \quad \Delta \mathbf{z} = \begin{bmatrix} \Delta \mathbf{z}_1 & \Delta \mathbf{z}_2 & \cdots & \Delta \mathbf{z}_{\frac{d_1}{b}} \end{bmatrix},$$

where b is the block size and b need to be a common divisor of d_1 and d_2 . We will need $\frac{d_1 d_2}{b^2}$ convolution kernels to densely connect these blocks, which can be expressed in math as

$$\Delta \mathbf{z}_i = \sum_{j=1}^{\frac{d_2}{b}} \Delta \mathbf{w}_{ij} \star \mathbf{x}_j, i \in \{1, 2, \dots, \frac{d_1}{b}\}.$$

This calculation can be represented by a block-circular matrix:

$$\Delta \mathbf{z} = \mathcal{C}_{\text{blk}}(\Delta \mathbf{w})\mathbf{x}, \quad \mathcal{C}_{\text{blk}}(\Delta \mathbf{w}) = \begin{bmatrix} \mathcal{C}(\Delta \mathbf{w}_{11}) & \mathcal{C}(\Delta \mathbf{w}_{12}) & \cdots & \mathcal{C}(\Delta \mathbf{w}_{1\frac{d_2}{b}}) \\ \mathcal{C}(\Delta \mathbf{w}_{21}) & \mathcal{C}(\Delta \mathbf{w}_{22}) & \cdots & \mathcal{C}(\Delta \mathbf{w}_{2\frac{d_2}{b}}) \\ \cdots & \cdots & \cdots & \cdots \\ \mathcal{C}(\Delta \mathbf{w}_{\frac{d_1}{b}1}) & \mathcal{C}(\Delta \mathbf{w}_{\frac{d_1}{b}2}) & \cdots & \mathcal{C}(\Delta \mathbf{w}_{\frac{d_1}{b}\frac{d_2}{b}}) \end{bmatrix}.$$

In this case, $\Delta \mathbf{w}_{ij} \in \mathbb{R}^b$ and we have $\frac{d_1 d_2}{b^2} b = \frac{d_1 d_2}{b}$ learnable parameters. In fact, b acts as a hyperparameter controlling the number of learnable parameters, just like r for LoRA. However, we highlight that while r controls the rank of the delta matrix and learnable parameter number at the same time, b only affects the latter. Disentangling these attributes enables higher adaptation flexibility and potential better results.

3.5 COMPLEXITY ANALYSIS

We compare the time complexity and space complexity of LoRA, VeRA and C³A in Table 1. Detailed analysis follows in this section.

3.5.1 TIME COMPLEXITY

LoRA incorporates low-rank matrices \mathbf{A} and \mathbf{B} , which are sequentially multiplied with the activation vector, resulting in a time complexity of $\mathcal{O}(r(d_1 + d_2))$. Typically, $r \ll \min(d_1, d_2)$. Conversely, VeRA, despite its high-rank nature and minimal number of trainable parameters, incurs a prohibitive time complexity of $\mathcal{O}(r_v(d_1 + d_2))$, where r_v can exceed $\max(d_1, d_2)$. Therefore, striking a balance between high rank and computational efficiency is never a low-hanging fruit.

Thanks to the $\mathcal{O}(n \log n)$ complexity of the FFT algorithm used in Equation 1, C^3A achieves a time complexity of $\mathcal{O}((d_1 + d_2) \log b + \frac{d_1 d_2}{b})$. The first term is the time complexity for FFT, and the second term is for aggregation. In practical scenarios, b is chosen as the greatest common divisor of d_1 and d_2 to achieve a high compression ratio. Given that, C^3A is comparable to LoRA in terms of time complexity.

3.5.2 SPACE COMPLEXITY

We analyze the space complexity of LoRA, VeRA, and C^3A during training. The differences among these methods primarily arise from the trainable parameters and the auxiliary tensors required for the forward pass and backpropagation. LoRA does not rely on auxiliary tensors, while VeRA necessitates 2 random projection matrices, with a total size of $r_v(d_1 + d_2)$. Since r_v is by no means negligible, the memory consumption of VeRA would be significantly larger than that of LoRA.

Table 1: Time and space complexity comparison of LoRA, VeRA and C^3A . We split the space complexity into Parameter number and Other auxiliary tensors to help better understand the differences. We highlight that in practice, to achieve similar performance, $\frac{\max(d_1, d_2)}{b} \leq r \ll r_v$.

Method	Time	# Param	# Other	# Total
LoRA	$\mathcal{O}(r(d_1 + d_2))$	$r(d_1 + d_2)$	0	$r(d_1 + d_2)$
VeRA	$\mathcal{O}(r_v(d_1 + d_2))$	$r_v + d_1$	$r_v(d_1 + d_2)$	$r_v(d_1 + d_2) + r_v + d_1$
C^3A	$\mathcal{O}((d_1 + d_2) \log b + \frac{d_1 d_2}{b})$	$\frac{d_1 d_2}{b}$	b	$\frac{d_1 d_2}{b} + b$

In terms of C^3A , the only additional auxiliary tensor would be of size $b \leq \min(d_1, d_2)$, which is reserved by the FFT algorithm. Given a proper b , which is often close to the greatest common divisor of d_1 and d_2 , the space complexity of C^3A excels. Additionally, we observe that when applying FFT, input blocks and output blocks are independent within their own group. Therefore, parallelization can be employed to enable the flexibility of trading space for time.

4 EXPERIMENT

In this section, we firstly conduct experiments on a synthetic dataset to show the superior expressiveness of C^3A over LoRA. After that, we comprehensively evaluate C^3A in both natural language processing (NLP) and computer vision (CV). For NLP, we first demonstrate the effectiveness of C^3A using the GLUE benchmark with RoBERTa-Base and RoBERTa-Large models. Additionally, we apply C^3A to fine-tuning the LLaMA family models, which stands as a representative of prevalent large language models (LLMs). For CV, we examine the most representative classification task using Vision Transformers (ViTs) on a wide range of datasets.

4.1 SYNTHETIC DATA

Settings. We distribute 8 points evenly on a 2D plane as cluster centers and randomly sample 30 points from 8 corresponding multivariate Gaussian distributions. A 3-layer MLP is then used to classify these point clusters. To compare the expressiveness of 2 types of layers, we replace the middle layer with either a low-rank layer or a circulant layer, ensuring that both layers have the same number of trainable parameters for a fair comparison.

Results. The results are presented in Figure 3. We observe that $LoRA_{r=1}$ struggles with this straightforward classification task. In contrast, $C^3A_{b=128/2}$, despite using the same number of parameters, achieves perfect classification, comparable to a standard linear layer. This demonstrates the high expressiveness of C^3A given the same parameter budget.

4.2 NATURAL LANGUAGE UNDERSTANDING

Baselines. We compare our C^3A with several representative PEFT methods, including BitFit Zaken et al. (2021), (IA)³ Liu et al. (2022), LoRA Hu et al. (2021), VeRA Kopiczko et al. (2023), and BOFT Liu et al. (2023). BitFit selectively fine-tunes existing parameters, specifically the biases. (IA)³ is the state-of-the-art method that adds extra adapters. LoRA is a widely known PEFT method that

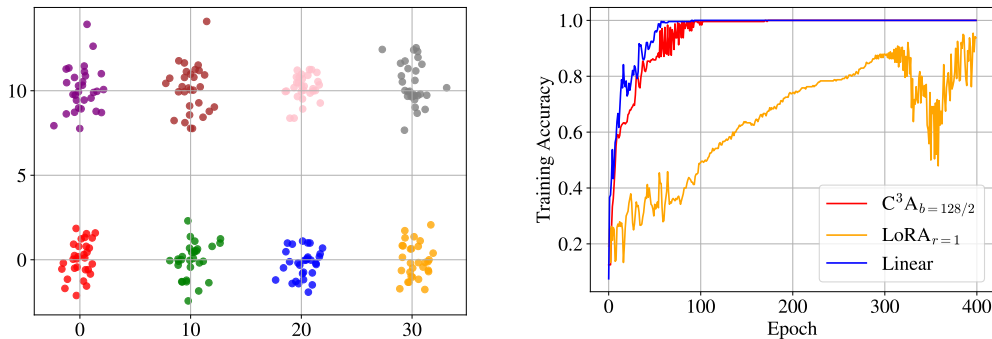


Figure 3: Expressiveness test on synthetic data. The left figure shows the synthetic data used for the experiment, while the right figure illustrates the training accuracy curves of a 3-layer MLP, incorporating C^3A , LoRA, and standard linear layers, respectively.

employs low-rank decomposition to compress additive delta matrices. VeRA is a recent approach that focuses on further reducing trainable parameters of LoRA while preserving a high rank. BOFT is another innovative method in PEFT research, compressing multiplicative delta matrices using orthogonal decomposition and butterfly factorization.

Table 2: Performance of different PEFT methods on the GLUE benchmark. We fine-tune pre-trained RoBERTa-Base and -Large models on 6 datasets. We report the Matthew’s Correlation Coefficient (MCC) for CoLA, Pearson Correlation Coefficient (PCC) for STS-B, and accuracy (Acc.) for all the remaining tasks. For each metric, a higher score indicates better performance. “Avg.” denotes the average score of each method across all datasets. The best results for each dataset are highlighted in **bold**. # Trainable parameters does not include the classification head since each method uses a head of the same size. Memory Cost is measured on fixed length (*i.e.*, 256) data with a batchsize of 64.

	Method	# Trainable Parameters	Memory Cost (GB)	SST-2	MRPC	CoLA	QNLI	RTE	STS-B	Avg.
BASE	Full	124M	17.19	94.01 \pm 0.39	87.10 \pm 0.79	62.00 \pm 1.16	92.40 \pm 0.28	77.33 \pm 2.68	90.70 \pm 0.14	83.92
	BitFit	102K	12.60	93.30 \pm 0.30	85.80 \pm 0.21	59.21 \pm 1.74	91.96 \pm 0.18	73.07 \pm 1.34	90.18 \pm 0.17	82.25
	(IA) ³	111K	19.86	92.98 \pm 0.34	85.86 \pm 0.59	60.49 \pm 1.09	91.56 \pm 0.17	69.10 \pm 1.18	90.06 \pm 0.21	81.67
	LoRA _{r=8}	295K	13.75	94.50 \pm 0.41	85.68 \pm 0.74	60.95 \pm 1.57	92.54 \pm 0.20	76.68 \pm 1.42	89.76 \pm 0.39	83.35
	VeRA _{r=1024}	43K	15.51	93.97 \pm 0.17	86.23 \pm 0.41	62.24 \pm 1.91	91.85 \pm 0.17	75.74 \pm 1.56	90.27 \pm 0.25	83.38
	BOFT _{b=8} ^{m=2}	166K	13.11	93.23 \pm 0.50	84.37 \pm 0.54	59.50 \pm 1.25	91.69 \pm 0.12	74.22 \pm 0.84	89.63 \pm 0.37	82.11
	$C^3A_{b=768/1}$	18K	12.83	93.42 \pm 0.26	86.33 \pm 0.32	61.83 \pm 0.96	91.83 \pm 0.04	76.17 \pm 1.39	90.46 \pm 0.29	83.34
	$C^3A_{b=768/6}$	111K	12.72	94.20 \pm 0.16	86.67 \pm 0.54	62.48 \pm 1.20	92.32 \pm 0.25	77.18 \pm 1.41	90.16 \pm 0.42	83.84
	LARGE	BitFit	271K	30.65	95.09 \pm 0.27	88.10 \pm 0.76	65.40 \pm 0.76	94.06 \pm 0.14	82.60 \pm 1.15	91.73 \pm 0.20
(IA) ³		295K	48.81	95.32 \pm 0.20	87.06 \pm 0.57	66.52 \pm 1.10	94.18 \pm 0.15	84.33 \pm 2.38	91.58 \pm 0.39	86.50
LoRA _{r=8}		786K	34.12	95.53 \pm 0.35	86.12 \pm 3.22	65.16 \pm 0.76	93.73 \pm 0.30	83.75 \pm 0.51	91.46 \pm 0.21	85.96
VeRA _{r=256}		61K	34.16	95.83 \pm 0.43	87.72 \pm 0.55	63.66 \pm 1.45	94.11 \pm 0.20	83.03 \pm 1.65	91.12 \pm 0.37	85.91
BOFT _{b=8} ^{m=2}		442K	33.08	95.76 \pm 0.41	88.28 \pm 0.33	64.72 \pm 2.37	93.89 \pm 0.14	82.82 \pm 1.40	91.03 \pm 0.32	86.08
$C^3A_{b=1024/1}$		49K	31.83	95.78 \pm 0.05	88.02 \pm 0.62	66.59 \pm 1.20	94.22 \pm 0.25	82.89 \pm 0.67	91.86 \pm 0.14	86.56
$C^3A_{b=1024/8}$		393K	31.79	95.78 \pm 0.15	88.09 \pm 0.47	67.18 \pm 1.92	94.26 \pm 0.19	84.62 \pm 1.36	91.81 \pm 0.36	86.96

Settings. We evaluate our proposed C^3A on the General Language Understanding Evaluation (GLUE) benchmark Wang et al. (2018), which encompasses a wide range of natural language understanding (NLU) tasks, including single-sentence classification, similarity and paraphrase, and natural language inference. To enhance practicality, we split these datasets following the train-validation-test approach. The best-performing model is selected based on validation set performance across the fine-tuning epochs, and the reported performance corresponds to its performance on the test set. For this evaluation, we fine-tune the pre-trained RoBERTa-Base and RoBERTa-Large models Liu et al. (2019). For the unique hyperparameters of different baselines, we adopt the values suggested in the original papers (*e.g.*, VeRA’s r and BOFT’s b and m). The number of trainable parameters excludes the classification head, as each method uses one of the same size. The shared hyperparameters (*i.e.*, the learning rate for classification head and for other trainable parameters, separately) are found by hyperparameter search. For the memory cost, to ensure fairness and consistency, we fix the length of input data to 256 tokens and use a batchsize of 64.

Results. Results are summarized in Table 2. In general, $C^3A_{b=768/1}$ and $C^3A_{b=1024/1}$ achieves better or on-par performance compared to baseline methods with extremely small trainable parameters. When a larger number of trainable parameters is allowed, $C^3A_{b=768/6}$ and $C^3A_{b=1024/8}$ significantly outperform baselines. In addition, compared to (IA)³, LoRA, VeRA, and BOFT, despite training a similar number of or more parameters, C^3A stands out for its excellent memory efficiency. The only method with better memory efficiency is BitFit, which can be seen as an upper bound since it does not introduce any new parameters. Furthermore, nearly all circulant delta matrices discovered by C^3A are full rank, indicating maximal capacity Zeng & Lee (2023) and providing theoretical support for the impressive results.

4.3 INSTRUCTION TUNING

Settings. We evaluate C^3A against LoRA by fine-tuning LLaMA2-7B/13B and LLaMA3-8B on 4 standard instruction tuning datasets: GSM8k Cobbe et al. (2021), MATH Yu et al. (2023), ViGGO Juraska et al. (2019), and SQL Zhong et al. (2017), following the setting outlined in Nikdan et al. (2024). For the SQL dataset, we preprocess by selecting 12.5% of the dataset, followed by an 4:1 train-test split. To ensure a fair comparison, we maintain LoRA parameters with $r = 32$ and a dropout rate of 0.05, while exploring various α values ranging from 32 to 128. All experiments are conducted for a standard single pass (epoch) over the dataset.

Results. In Table 3, we summarize our main experiments. It can be observed that C^3A generally surpasses LoRA across both LLaMA2-7B/13B and LLaMA3-8B. Notably, C^3A only utilizes less than half of the parameter count compared to LoRA. Overall, these results clearly highlight the effectiveness of C^3A .

Table 3: Comparison of C^3A and LoRA on fine-tuning LLaMA2 and LLaMA3 models in terms of accuracy and trainable parameters. The best results for each dataset are highlighted in **bold**. ‘‘Avg.’’ denotes the average accuracy of each method across all datasets.

Model	Method	# Trainable Parameters	GSM8k	MATH	ViGGO	SQL	Avg.
LLaMA2-7B	LoRA _{r=32}	16.8M	27.22	4.10	92.24	65.39	47.24
	$C^3A_{b=4096/32}$	8.4M	29.34	4.25	94.03	66.21	48.46
LLaMA2-13B	LoRA _{r=32}	26.2M	42.68	6.70	93.19	67.53	52.53
	$C^3A_{b=5120/32}$	13.1M	42.00	6.65	95.57	67.28	52.88
LLaMA3-8B	LoRA _{r=32}	13.6M	56.57	18.95	91.78	68.19	58.87
	$C^3A_{b=4096/32}$	5.2M	57.54	19.75	93.07	69.47	59.96

4.4 IMAGE CLASSIFICATION

Settings. We focus on the task of image classification utilizing the Vision Transformer (ViT) models. Specifically, we employ both the Base and Large variants of this prevalent computer vision foundation model, as introduced by Dosovitskiy et al. (2020). These ViT models are pre-trained on the extensive ImageNet-21K dataset Ridnik et al. (2021). For the fine-tuning phase, we utilize a diverse set of datasets including Pets, Cars, DTD, EuroSAT, FGVC and RESISC.

Results. Table 4 presents a summary of the results obtained from 6 image classification datasets using the ViT Base and Large models. The LoRA and C^3A methods both show substantial performance improvements over Head Tuning, highlighting their effectiveness in the image classification domain. Notably, our method achieves comparable performance to LoRA while utilizing only half of the parameter count.

5 CONCLUSION

In this paper, we introduce C^3A , an innovative approach to Parameter-Efficient Fine-Tuning (PEFT). Unlike LoRA, which utilizes low-rank decomposition, C^3A employs circular convolution and its associated circulant matrix to model the delta weight matrix. This approach aims to decouple the

Table 4: Fine-tuning results with ViT-Base and ViT-Large models on various image classification datasets. The models are fine-tuned for 10 epochs, and the best-performing model, based on validation set accuracy, is selected. The reported accuracy corresponds to the performance on the test set. The best results for each dataset are highlighted in **bold**. “Avg.” denotes the average accuracy of each method across all datasets.

	Method	# Trainable Parameters	Pets	Cars	DTD	EuroSAT	FGVC	RESISC	Avg.
BASE	Head	-	90.28 \pm 0.43	25.76 \pm 0.28	69.77 \pm 0.67	88.72 \pm 0.13	17.44 \pm 0.43	74.22 \pm 0.10	61.03
	Full	85.8M	92.82 \pm 0.54	85.10 \pm 0.21	80.11 \pm 0.56	99.11 \pm 0.07	61.60 \pm 1.00	96.00 \pm 0.23	85.79
	LoRA $_{r=16}$	590K	93.76 \pm 0.44	78.04 \pm 0.33	78.56 \pm 0.62	98.84 \pm 0.08	56.64 \pm 0.55	94.66 \pm 0.17	83.42
	C ³ A $_{b=768/12}$	221K	93.88 \pm 0.22	79.05 \pm 0.35	80.57 \pm 0.53	98.88 \pm 0.07	54.31 \pm 0.79	94.54 \pm 0.23	83.54
LARGE	Head	-	91.11 \pm 0.30	37.91 \pm 0.27	73.33 \pm 0.26	92.64 \pm 0.08	24.62 \pm 0.24	82.02 \pm 0.11	66.94
	Full	303M	94.30 \pm 0.31	88.15 \pm 0.50	80.18 \pm 0.66	99.06 \pm 0.10	67.38 \pm 1.06	96.08 \pm 0.20	87.53
	LoRA $_{r=16}$	1.57M	94.62 \pm 0.47	86.11 \pm 0.42	80.09 \pm 0.42	98.99 \pm 0.03	63.64 \pm 0.83	95.94 \pm 0.21	86.56
	C ³ A $_{b=1024/16}$	786K	94.48 \pm 0.30	84.94 \pm 0.39	82.62 \pm 0.52	98.75 \pm 0.19	63.80 \pm 0.37	95.52 \pm 0.16	86.69

rank of the delta weight matrix from the number of learnable parameters, allowing for high-rank adaptation while maintaining a limited parameter size. By leveraging the Fast Fourier Transform (FFT) in both the forward and backward passes, C³A achieves significant computational and memory efficiency. Consequently, C³A presents itself as a compelling alternative to LoRA for model fine-tuning.

REFERENCES

- Bassam Bamieh. Discovering transforms: A tutorial on circulant matrices, circular convolution, and the discrete fourier transform. *arXiv preprint arXiv:1805.05533*, 2018.
- Tom Brown, Benjamin Mann, Nick Ryder, Melanie Subbiah, Jared D Kaplan, Prafulla Dhariwal, Arvind Neelakantan, Pranav Shyam, Girish Sastry, Amanda Askell, et al. Language models are few-shot learners. *Advances in neural information processing systems*, 33:1877–1901, 2020.
- Aochuan Chen, Yuguang Yao, Pin-Yu Chen, Yihua Zhang, and Sijia Liu. Understanding and improving visual prompting: A label-mapping perspective. In *Proceedings of the IEEE/CVF Conference on Computer Vision and Pattern Recognition*, pp. 19133–19143, 2023.
- Yu Cheng, Felix X Yu, Rogerio S Feris, Sanjiv Kumar, Alok Choudhary, and Shi-Fu Chang. An exploration of parameter redundancy in deep networks with circulant projections. In *Proceedings of the IEEE international conference on computer vision*, pp. 2857–2865, 2015.
- Karl Cobbe, Vineet Kosaraju, Mohammad Bavarian, Mark Chen, Heewoo Jun, Lukasz Kaiser, Matthias Plappert, Jerry Tworek, Jacob Hilton, Reiichiro Nakano, et al. Training verifiers to solve math word problems. *arXiv preprint arXiv:2110.14168*, 2021.
- Caiwen Ding, Siyu Liao, Yanzhi Wang, Zhe Li, Ning Liu, Youwei Zhuo, Chao Wang, Xuehai Qian, Yu Bai, Geng Yuan, Xiaolong Ma, Yipeng Zhang, Jian Tang, Qinru Qiu, Xue Lin, and Bo Yuan. Circnn: accelerating and compressing deep neural networks using block-circulant weight matrices. In *Proceedings of the 50th Annual IEEE/ACM International Symposium on Microarchitecture, MICRO-50 ’17*, pp. 395–408, New York, NY, USA, 2017. Association for Computing Machinery. ISBN 9781450349529. doi: 10.1145/3123939.3124552. URL <https://doi.org/10.1145/3123939.3124552>.
- Alexey Dosovitskiy, Lucas Beyer, Alexander Kolesnikov, Dirk Weissenborn, Xiaohua Zhai, Thomas Unterthiner, Mostafa Dehghani, Matthias Minderer, Georg Heigold, Sylvain Gelly, et al. An image is worth 16x16 words: Transformers for image recognition at scale. *arXiv preprint arXiv:2010.11929*, 2020.
- Morris Dworkin, Elaine Barker, James Nechvatal, James Foti, Lawrence Bassham, E. Roback, and James Dray. Advanced encryption standard (aes), 2001-11-26 2001.

-
- Zihao Fu, Haoran Yang, Anthony Man-Cho So, Wai Lam, Lidong Bing, and Nigel Collier. On the effectiveness of parameter-efficient fine-tuning. In *Proceedings of the AAAI conference on artificial intelligence*, volume 37, pp. 12799–12807, 2023.
- Tianyu Gao, Adam Fisch, and Danqi Chen. Making pre-trained language models better few-shot learners. *arXiv preprint arXiv:2012.15723*, 2020.
- Gene H. Golub and Charles F. Van Loan. *Matrix computations (3rd ed.)*. Johns Hopkins University Press, USA, 1996. ISBN 0801854148.
- Yanwei Gong, Xiaolin Chang, Jelena Mišić, Vojislav B Mišić, Jianhua Wang, and Haoran Zhu. Practical solutions in fully homomorphic encryption: a survey analyzing existing acceleration methods. *Cybersecurity*, 7(1):5, 2024.
- Demi Guo, Alexander M Rush, and Yoon Kim. Parameter-efficient transfer learning with diff pruning. *arXiv preprint arXiv:2012.07463*, 2020.
- Song Han, Huizi Mao, and William J Dally. Deep compression: Compressing deep neural networks with pruning, trained quantization and huffman coding. *arXiv preprint arXiv:1510.00149*, 2015.
- Junxian He, Chunting Zhou, Xuezhe Ma, Taylor Berg-Kirkpatrick, and Graham Neubig. Towards a unified view of parameter-efficient transfer learning. *arXiv preprint arXiv:2110.04366*, 2021.
- Edward J Hu, Yelong Shen, Phillip Wallis, Zeyuan Allen-Zhu, Yanzhi Li, Shean Wang, Lu Wang, and Weizhu Chen. Lora: Low-rank adaptation of large language models. *arXiv preprint arXiv:2106.09685*, 2021.
- A. W. Ingleton. The rank of circulant matrices. *Journal of the London Mathematical Society*, s1-31(4):445–460, 1956. doi: <https://doi.org/10.1112/jlms/s1-31.4.445>. URL <https://londmathsoc.onlinelibrary.wiley.com/doi/abs/10.1112/jlms/s1-31.4.445>.
- Juraj Juraska, Kevin K Bowden, and Marilyn Walker. Viggo: A video game corpus for data-to-text generation in open-domain conversation. *arXiv preprint arXiv:1910.12129*, 2019.
- Alexander Kirillov, Eric Mintun, Nikhila Ravi, Hanzi Mao, Chloe Rolland, Laura Gustafson, Tete Xiao, Spencer Whitehead, Alexander C Berg, Wan-Yen Lo, et al. Segment anything. In *Proceedings of the IEEE/CVF International Conference on Computer Vision*, pp. 4015–4026, 2023.
- Dawid Jan Kopiczko, Tijmen Blankevoort, and Yuki Markus Asano. Vera: Vector-based random matrix adaptation. *arXiv preprint arXiv:2310.11454*, 2023.
- Changli Li, Hon Keung Kwan, and Xinxin Qin. Revisiting linear convolution, circular convolution and their related methods. *2020 13th International Congress on Image and Signal Processing, BioMedical Engineering and Informatics (CISP-BMEI)*, pp. 1124–1131, 2020. URL <https://api.semanticscholar.org/CorpusID:227220098>.
- Xiang Lisa Li and Percy Liang. Prefix-tuning: Optimizing continuous prompts for generation. *arXiv preprint arXiv:2101.00190*, 2021.
- Yuhan Li, Peisong Wang, Zhixun Li, Jeffrey Xu Yu, and Jia Li. Zerog: Investigating cross-dataset zero-shot transferability in graphs. *arXiv preprint arXiv:2402.11235*, 2024.
- Haokun Liu, Derek Tam, Mohammed Muqeeth, Jay Mohta, Tenghao Huang, Mohit Bansal, and Colin A Raffel. Few-shot parameter-efficient fine-tuning is better and cheaper than in-context learning. *Advances in Neural Information Processing Systems*, 35:1950–1965, 2022.
- Shih-Yang Liu, Chien-Yi Wang, Hongxu Yin, Pavlo Molchanov, Yu-Chiang Frank Wang, Kwang-Ting Cheng, and Min-Hung Chen. Dora: Weight-decomposed low-rank adaptation. *arXiv preprint arXiv:2402.09353*, 2024.
- Weiyang Liu, Zeju Qiu, Yao Feng, Yuliang Xiu, Yuxuan Xue, Longhui Yu, Haiwen Feng, Zhen Liu, Juyeon Heo, Songyou Peng, et al. Parameter-efficient orthogonal finetuning via butterfly factorization. *arXiv preprint arXiv:2311.06243*, 2023.

-
- Yinhan Liu, Myle Ott, Naman Goyal, Jingfei Du, Mandar Joshi, Danqi Chen, Omer Levy, Mike Lewis, Luke Zettlemoyer, and Veselin Stoyanov. Roberta: A robustly optimized bert pretraining approach. *arXiv preprint arXiv:1907.11692*, 2019.
- Sadhika Malladi, Tianyu Gao, Eshaan Nichani, Alex Damian, Jason D Lee, Danqi Chen, and Sanjeev Arora. Fine-tuning language models with just forward passes. *Advances in Neural Information Processing Systems*, 36:53038–53075, 2023.
- Sourab Mangrulkar, Sylvain Gugger, Lysandre Debut, Younes Belkada, Sayak Paul, and Benjamin Bossan. Peft: State-of-the-art parameter-efficient fine-tuning methods. <https://github.com/huggingface/peft>, 2022.
- Clare D. McGillem and George R. Cooper. Continuous and discrete signal and system analysis. 1984. URL <https://api.semanticscholar.org/CorpusID:117907785>.
- Mahdi Nikdan, Soroush Tabesh, and Dan Alistarh. Rosa: Accurate parameter-efficient fine-tuning via robust adaptation. *arXiv preprint arXiv:2401.04679*, 2024.
- Jaehoon Oh, Hyungjun Yoo, ChangHwan Kim, and Se-Young Yun. Boil: Towards representation change for few-shot learning. *arXiv preprint arXiv:2008.08882*, 2020.
- Zeju Qiu, Weiyang Liu, Haiwen Feng, Yuxuan Xue, Yao Feng, Zhen Liu, Dan Zhang, Adrian Weller, and Bernhard Schölkopf. Controlling text-to-image diffusion by orthogonal finetuning. *Advances in Neural Information Processing Systems*, 36:79320–79362, 2023.
- L. R. Rabiner, B. Gold, and C. K. Yuen. Theory and application of digital signal processing. *IEEE Transactions on Systems, Man, and Cybernetics*, 8(2):146–146, 1978. doi: 10.1109/TSMC.1978.4309918.
- Alec Radford, Jong Wook Kim, Chris Hallacy, Aditya Ramesh, Gabriel Goh, Sandhini Agarwal, Girish Sastry, Amanda Askell, Pamela Mishkin, Jack Clark, et al. Learning transferable visual models from natural language supervision. In *International conference on machine learning*, pp. 8748–8763. PMLR, 2021.
- Sylvestre-Alvise Rebuffi, Hakan Bilen, and Andrea Vedaldi. Learning multiple visual domains with residual adapters. *Advances in neural information processing systems*, 30, 2017.
- Tal Ridnik, Emanuel Ben-Baruch, Asaf Noy, and Lihi Zelnik-Manor. Imagenet-21k pretraining for the masses. *arXiv preprint arXiv:2104.10972*, 2021.
- Andreas Rücklé, Gregor Geigle, Max Glockner, Tilman Beck, Jonas Pfeiffer, Nils Reimers, and Iryna Gurevych. Adapterdrop: On the efficiency of adapters in transformers. *arXiv preprint arXiv:2010.11918*, 2020.
- Hugo Touvron, Thibaut Lavril, Gautier Izacard, Xavier Martinet, Marie-Anne Lachaux, Timothée Lacroix, Baptiste Rozière, Naman Goyal, Eric Hambro, Faisal Azhar, et al. Llama: Open and efficient foundation language models. *arXiv preprint arXiv:2302.13971*, 2023.
- Alex Wang, Amanpreet Singh, Julian Michael, Felix Hill, Omer Levy, and Samuel R Bowman. Glue: A multi-task benchmark and analysis platform for natural language understanding. *arXiv preprint arXiv:1804.07461*, 2018.
- Runxin Xu, Fuli Luo, Zhiyuan Zhang, Chuanqi Tan, Baobao Chang, Songfang Huang, and Fei Huang. Raise a child in large language model: Towards effective and generalizable fine-tuning. *arXiv preprint arXiv:2109.05687*, 2021.
- Felix Yu, Sanjiv Kumar, Yunchao Gong, and Shih-Fu Chang. Circulant binary embedding. In *International conference on machine learning*, pp. 946–954. PMLR, 2014.
- Longhui Yu, Weisen Jiang, Han Shi, Jincheng Yu, Zhengying Liu, Yu Zhang, James T Kwok, Zhenguang Li, Adrian Weller, and Weiyang Liu. Metamath: Bootstrap your own mathematical questions for large language models. *arXiv preprint arXiv:2309.12284*, 2023.

-
- Shen Yuan, Haotian Liu, and Hongteng Xu. Bridging the gap between low-rank and orthogonal adaptation via householder reflection adaptation. *arXiv preprint arXiv:2405.17484*, 2024.
- Elad Ben Zaken, Shauli Ravfogel, and Yoav Goldberg. Bitfit: Simple parameter-efficient fine-tuning for transformer-based masked language-models. *arXiv preprint arXiv:2106.10199*, 2021.
- Yuchen Zeng and Kangwook Lee. The expressive power of low-rank adaptation. *arXiv preprint arXiv:2310.17513*, 2023.
- Yihua Zhang, Hongkang Li, Yuguang Yao, Aochuan Chen, Shuai Zhang, Pin-Yu Chen, Meng Wang, and Sijia Liu. Visual prompting reimagined: The power of activation prompts, 2024a. URL <https://openreview.net/forum?id=0b328CMwn1>.
- Yushun Zhang, Congliang Chen, Ziniu Li, Tian Ding, Chenwei Wu, Yinyu Ye, Zhi-Quan Luo, and Ruoyu Sun. Adam-mini: Use fewer learning rates to gain more. *arXiv preprint arXiv:2406.16793*, 2024b.
- Victor Zhong, Caiming Xiong, and Richard Socher. Seq2sql: Generating structured queries from natural language using reinforcement learning. *arXiv preprint arXiv:1709.00103*, 2017.